NOTE *Surgery*

Diffuse idiopathic skeletal hyperostosis with prominent appendicular bone proliferation in a dog

Juyeon OH[1)], Ju-Hwan LEE[2)], Kyoung-Oh CHO[1)] and Jihye CHOI[1)]*

[1)]*College of Veterinary Medicine, Chonnam National University, Gwangju 500-757, South Korea*
[2)]*Chonnam National University Veterinary Teaching Hospital, Gwangju 500-757, South Korea*

(Received 6 March 2014/Accepted 12 December 2014/Published online in J-STAGE 10 January 2015)

ABSTRACT. This report described radiographic and CT features of atypical diffuse idiopathic skeletal hyperostosis in a 5 year-old, female Shih-tzu showing marked proliferative bone lesions in the appendicular skeleton with minor spinal changes. Continuous or flowing bony bridge formation of vertebrae is used as the gold standard for diagnosing diffuse idiopathic skeletal hyperostosis. However, this criterion seems not to be suitable for appendicular type diffuse idiopathic skeletal hyperostosis, as in the present case. Diffuse idiopathic skeletal hyperostosis is a progressive skeletal disease, and thus, enthesophytosis and the multiple bony proliferations at insertion sites of ligaments and tendons to appendicular bones in a lamellar or trabecular pattern were considered diagnostic features of the appendicular type of diffuse idiopathic skeletal hyperostosis.

KEY WORDS: appendicular, canine, CT, diffuse idiopathic skeletal hyperostosis

doi: 10.1292/jvms.14-0115; *J. Vet. Med. Sci.* 77(4): 493–497, 2015

Diffuse idiopathic skeletal hyperostosis is a systemic disease affecting the axial and appendicular skeletons of humans and dogs [8, 12, 13]. In particular, several cases involving spinal sites have been reported [2–5, 9]. In human medicine, three radiographic criteria for differentiating diffuse idiopathic skeletal hyperostosis from other proliferative spinal diseases, such as spondylosis deformans, osteochondrosis and ankylosing spondylitis, have been presented. These include: (1) flowing calcification and ossification along the ventrolateral aspect of at least four continuous vertebral bodies, with or without localized pointed excrescences at the inventing vertebral body-intervertebral disc junctions, (2) relative preservation of disc width and the absence of extensive changes of degenerative disc disease and (3) absence of apophyseal joint ankylosis and sacroiliac joint erosion, sclerosis or intra-articular fusion [11]. These criteria are also used as the gold standard for diagnosing diffuse idiopathic skeletal hyperostosis in veterinary medicine. However, the early stages of diffuse idiopathic skeletal hyperostosis cannot be recognized from these criteria, because it is a progressive disease [7]. Diffuse idiopathic skeletal hyperostosis may occur in the appendicular skeleton with minor or absent abnormalities in the axial skeleton [11]. Therefore, these diffuse idiopathic skeletal hyperostosis criteria with spinal manifestations have limitations to fulfill the diagnosis of appendicular diffuse idiopathic skeletal hyperostosis. In this study, we described the diffuse idiopathic skeletal hyperostosis with prominent proliferative change from appendicular bones without typical vertebral lesions and suggested the diagnostic features for appendicular type of diffuse idiopathic skeletal hyperostosis.

A 5 year-old, female Shih-tzu presented with a recurrent generalized dermatologic disorder. A physical examination revealed keratosis, pyoderma and pigmentation over all of the skin, and restricted hip motion, with difficulty walking up and down stairs. No significant abnormalities in the complete blood count, electrolytes or serum chemistry were detected, including calcium (9.3 mg/d*l*; reference 7.9–12.0 mg/d*l*) and phosphate (4.7 mg/d*l*; reference 2.5–6.8 mg/d*l*). The values of free thyroxine (1.38 μg/d*l*; reference 0.6–3.7 μg/d*l*), thyroid stimulated hormone (0.166 μg/m*l*; reference 0.05–0.42 μg/m*l*) and total thyroxine (1.03 μg/d*l*; reference 1.0–4.0 μg/d*l*) were within the normal reference ranges.

Marked new bone formation with a smooth margin was observed over bilateral ilium and ischium on radiography, and relatively mild bony changes with a similar appearance were observed in the pubis. A lamellar periosteal reaction, which consisted of a radiolucent inner layer surrounded with a radiopaque outer layer, was observed along bilateral femurs and tibia. The outer radiopaque bone had similar bone density as cortical bone (Fig. 1). Additional radiographs to define the extent of the disease revealed bone proliferation with a smooth margin at the infraglenoid tubercle of the right scapula, surfaces of bilateral humeri, radii and ulna. In contrast, joints, such as the shoulder, elbow, hip, stifle, carpus and tarsus, were preserved with no evidence of bone formation. Bone with a smooth margin had proliferated from the spinous processes of all thoracic and lumbar vertebrae, the ventral surface of the vertebral body of the second and from the fourth to seventh lumbar vertebrae and the ribs. Although the ventral surface of vertebrae could not be definitely evaluated due to superimposition with the transverse processes,

*CORRESPONDENCE TO: CHOI, J., College of Veterinary Medicine, Chonnam National University, Yongbong-ro, Buk-gu, Gwangju, 500-757, South Korea. e-mail: imsono@chonnam.ac.kr

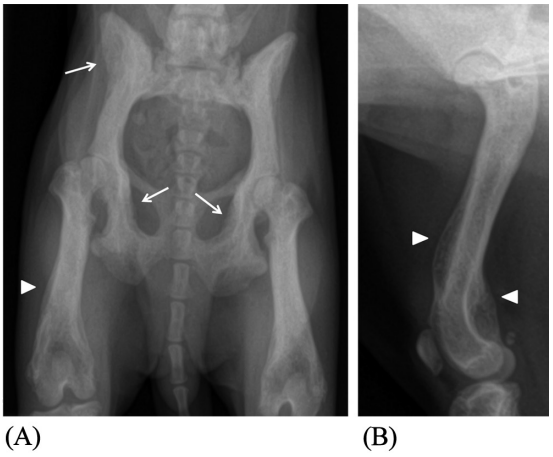

Fig. 1. Ventrodorsal (A) and right lateral (B) radiographs of the hindlimbs. Proliferative bony changes with a smooth margin were present over the entire ilium and ischium (white arrows). Periosteal reaction along the right and left femurs was observed as a laminated bone pattern that had radiolucent trabecular intensity surrounded by a radiopaque neocortex (arrowheads).

there was no continuous or flowing pattern of proliferative bones and no evidence of bone destruction. Intervertebral disc width was preserved (Fig. 2A).

CT was performed to investigate the extent and severity of bone changes in detail using a 16 channel multi-detector CT scanner (Siemens Emotion 16, Siemens, Forchheim, Germany). Helical CT scanning was performed from the cervix to the sacrum using 130 kVp and 200 mAs with a 1 mm slice thickness to acquire the vertebral CT images; from the thoracic and pelvic limbs with 130 kVp, 270 mAs and 1 mm slice thickness for the appendicular skeleton; and from the nostril to the occipital bones with 110 kVp, 130 mAs and a 1 mm slice thickness for the skull. Then, multiplanar reconstruction, curvilinear reconstruction and three dimensional volume rendering reconstruction were carried out. Transverse vertebral CT images showed irregular bone spurs at the ventral part of the sixth and seventh cervical and from the first to sixth thoracic vertebrae, and lamellar bone proliferation with outer hyperdense and inner hypodense composition on the ventral surface from the tenth to the thirteenth thoracic vertebrae and from the first to third lumbar region. More severe bone proliferation was shown in the ventral part of the fourth to seventh lumbar vertebrae as a remarkable trabecular bone pattern with neocortex formation. The distribution and proliferative pattern of new bone were more clearly described on the reconstructed sagittal plane showing bone formation mainly produced from the ventral surface of the vertebral body without bridge formation between adjacent vertebrae. That is, there was no continuous or flowing pattern of new bone between cranial and caudal vertebrae (Fig. 2B and 2C). Thickening of the spinous processes of thoracic and lumbar vertebrae was observed on the transverse and sagittal planes. The bone proliferative changes were more marked in most of the appendicular bones as an irregular and lacy pattern. The origins of the supraspinatus, infraspinatus and subscapularis muscles had irregular bony proliferation. Bilateral humeri had a relatively mild periosteal reaction with a lacy and irregular margin. Most parts of the radii showed lacy and irregular proliferation with the typical lamellar pattern from the distal diaphysis to epiphysis. Severe bone formation was found in most of the pelvis. In particular, new bone that proliferated in the iliac crest was thicker than normal bone. Bone formation around the dorsal sacroiliac ligament with fusion of the sacroiliac joint was detected on dorsal CT images. The ileal body at the origin of the deep gluteus muscle also showed severe proliferative changes, and the ischiatic tuberosity, where the sacrotuberous ligament was inserted, had distinct proliferation. Bilateral coxofemoral joints were preserved. Lamellar or trabecular bone formation was noted in the distal femur and proximal and distal tibiae (Fig. 3A–3E). CT images of the skull demonstrated no remarkable findings.

Proliferative changes in both the axial and appendicular skeletons except for the digits and skull were confirmed based on the radiographic and CT examinations. Various diseases, including hypertrophic osteopathy, osteopetrosis, vitamin A toxicity and thyroid acropachy were considered

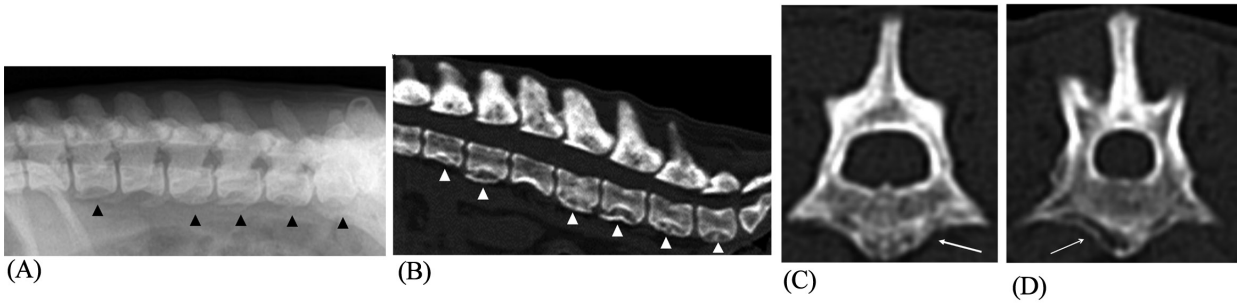

Fig. 2. Lateral radiography (A) and sagittal (B) CT image of the lumbar vertebra and transverse CT images of the second (C) and fourth (D) lumbar vertebrae. Bony proliferation on the ventral surface of the second and from the fourth to seventh lumbar vertebral bodies was observed, but was not distinct because of superimposition with the transverse processes on radiography (black arrowheads). A sagittal CT scan revealed more distinct proliferative bone formation on the ventral surface of the vertebral body (white arrowheads). Transverse images show a lamellar pattern with outer hyperdense and inner hypodense composition (white arrow) or more severe bone proliferation with a remarkable trabecular bone pattern and formation of neocortex.

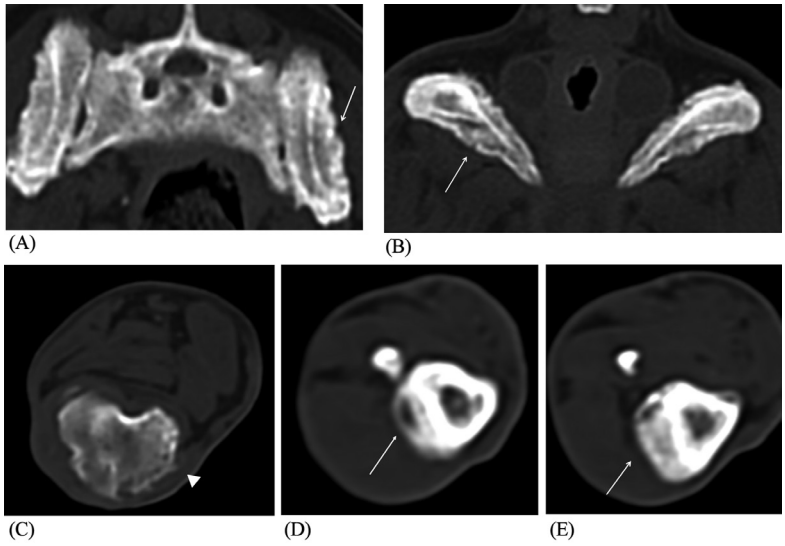

Fig. 3. Transverse CT image of appendicular bone including iliac crest inserted into the deep gluteal muscle; (A), ischiatic tuberosity inserted into the sacrotuberous ligament (B), right distal femur (C) and right distal tibia; (D, E) attached diverse ligaments and tendons. Relatively mild lesions show lacy and irregular bony changes (arrowhead). In addition, more progressive proliferation was noted as a laminated pattern and a trabecular bone pattern (white arrow).

in the differential diagnosis. Hypertrophic osteopathy is an osteoproductive disease, typically commencing on the distal extremities and extending proximally. This disease is radiographically characterized by a nodular or spiculated patterned periosteal reaction [1]. However, in this case, bilateral digits had no evidence of bony proliferation, and the new periosteal bone was in a lamellar or trabecular bone pattern. Osteopetrosis reveals increased bone opacity in medullary portions with normal shape and size of bone [10]. In this patient, the affected bones had relatively hypodense medullary portions, maintaining distinction from the hyperdense cortical bone. Vitamin A toxicity is one of the reasons for hyperostosis in cats, whereas it has an opposite effect in dogs and causes bone resorption [6]. Additionally, thyroid acropachy was ruled out, because the values of free thyroxine, thyroid stimulated hormone and total thyroxine were within the normal reference ranges. Consequently, it was difficult to make the initial diagnosis based on the diagnostic imaging.

The dog was euthanized at the owner's request in view of the uncertain prognosis and chronic dermatitis, and a necropsy was performed. New bone formation in the joint margins (osteophyte) and ligament and tendon insertion sites (enthesophytes) as well as periosteal reactions in both spinal and extraspinal structures was the most prominent features. Osteophytes and enthesophytes were arranged into small to sharp finger-like projections in the spinal column (Fig. 4). There was thickening of the dorsal spinous processes of vertebrae and irregular rib shapes. Enthesophytes appeared as mineral deposits around the joint surfaces as well as in the diaphyseal region of the humeri, radii, ulna, femurs and tibiae. These irregular mineral deposits varied from pinpoint size to several millimeters in diameter and were more obvious on the para-articular surfaces of the humeri, tibiae and femurs. Evident fusion of the sacroiliac joint and the periosteal reaction was seen, and it was more severe in the regions of the ilium and ischium; this finding was compatible with the three dimensional volume rendered CT images (Fig. 4A–4D).

A histopathologic examination was performed on the right forelimb and right hindlimb (Fig. 5). Osteoclasts were occasionally seen in the rough and thickened periosteal areas in the articular regions of the humeri and femurs. Along these osteoclasts, there were osteoblasts in the marginal area between the periosteum and subchondral bone. New bone formation, such as enthesophytes, was observed, resulting in distinct separation from cortical bone. Reactive bone was observed along the margins of the humeral and femoral articular surfaces. Masson's trichrome staining showed that these marginal areas had merged into a meshwork of dense collagen bundles. These collagen bundles were arranged randomly and made a dense meshwork parallel to the articular surface. In addition, the deep zonal area showed an irregular tidemark, calcified cartilage, mildly clustered chondrocytes and vascular invasion, indicating osteoarthritis. Based on these results, canine diffuse idiopathic skeletal hyperostosis was diagnosed.

In our case, intervertebral disc width was preserved without degenerative disc disease. The apophyseal and sacroiliac joints showed no evidence of ankylosis, erosion or sclerosis that met criteria (2) and (3). However, the proliferative bone lesion in vertebrae was mild without continuous or flowing ossification in the ventral region, which is a typical feature of diffuse idiopathic skeletal hyperostosis. Furthermore, accurate radiographic evaluation was difficult, because of superimposition with the surrounding structures, such as transverse processes.

The CT examination demonstrated the extent and severity

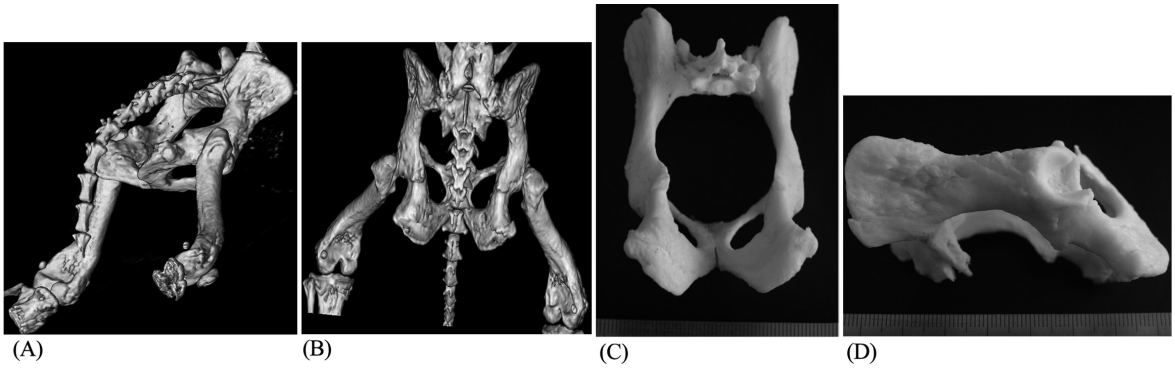

Fig. 4. Three dimensional volume rendering reconstructed image of the pelvis and bilateral femur (A, B). A severe periosteal reaction was seen not only in the macerated pelvis (C, D) but also on the three dimensional volume rendering reconstructed image.

of new bone formation. In particular, ventral bone formation of vertebrae was determined on the sagittal plane without superimposition, and there was no continuous bone bridge formation. However, the classical features of diffuse idiopathic skeletal hyperostosis, including the laminated bone pattern, consisting of a relative low density area between the ossified deposits and underlying vertebral body, was observed on transverse CT images. In some regions, such as the fourth to seventh lumbar vertebrae, more enlarged and thickened ossification, which was observed as a trabecular bony pattern, was found and was considered the more progressed lesion.

Diffuse idiopathic skeletal hyperostosis with appendicular manifestations has been reported in only two dogs, which were both 4-year-old and large breeds [8, 13]. Both dogs had a history of progressive gait abnormalities for the past 1–2 years, and they were euthanized because of extreme stiffness, pain and lack of a response to treatment [8, 13]. Long-term radiographic monitoring of bone lesions was performed in one of them for 26 months [13]. On the initial radiography, the periosteal reaction with a mottled appearance was observed in the proximal region of the right femur, ischium and ilium. Then, progressive ossification of the right elbow, pelvic, right stifle and tarsal joints occurred. Finally, the pelvis, femur and caudal lumbar vertebrae were osseously fused to show a trabecular pattern. Para-articular joint fusion around the elbow and smooth new bone formation in the stifle and tarsal joints developed progressively with preservation of the joint space itself. These characteristic radiographic findings were also observed in the other case [8]. Periarticular new bone and enthesiophytes were present in the bilateral shoulders and elbows, hip joint and the right stifle joint. However, both carpal and tarsal joints were normal [8]. In both cases, thin section radiography demonstrated a trabecular bone pattern in the neocortex [8, 13]. The regions of proliferative changes in appendicular bones of our case were similar to previous reports [8, 13]. Enthesiophyte, a bone spur at the sites of attachment of tendon and ligament, periarticular osteophytes and the periosteal reaction were prominently demonstrated with preservation of the joint surfaces including the shoulder, elbow, hip, stifle, carpus and tarsus. The severity of new bone formation in this patient was comparatively less than that in the previous cases showing mineralization of soft tissue with mottled opacity, progressive bony fusion and flowing ossification along the ventrolateral aspect of at least three continuous vertebral bodies. The present case did not have bony fusion or muscle mineralization, and proliferative changes in the vertebral body were not clearly identified on lateral radiographs. Diffuse idiopathic skeletal hyperostosis was estimated to be at the early stage based on only mild symptoms in our case.

The CT examination showed characteristic changes in the appendicular region in detail. The region of bone proliferation was identified exactly without superimposition using the dorsal and sagittal images from multiplanar reconstruction as well as the transverse images. Moreover, three dimensional volume rendering reconstructed images at various angles improved our understanding of the multiple proliferative lesions. Conspicuous bone proliferation was noted in regions of attachment to muscles, tendons and ligaments to bone including iliac crest, ileal body, sacroiliac joint, distal femurs, and proximal and distal tibiae. The definite features of bone proliferation in the appendicular region were evaluated with CT, although detailed slab radiography was not performed in this dog. The relatively mild proliferative lesions showed as lacy and irregular bony changes, and the laminated pattern and trabecular bone pattern were noted in regions with more severe proliferation.

This study describes the diagnostic radiography and CT features of canine diffuse idiopathic skeletal hyperostosis. Continuous flowing bone formation at the ventral region of the vertebral body has been used as a typical feature of diffuse idiopathic skeletal hyperostosis. However, this criterion seems not to be suitable for appendicular type of diffuse idiopathic skeletal hyperostosis, as in our case, showing marked proliferative bone lesions in the appendicular skeleton with minor spinal changes. We could not determine whether the discrepancy in vertebral lesions in this case as compared to the previous cases was related to the breed, because this case was the first small breed dog with diffuse idiopathic skeletal hyperostosis. The typical vertebral flowing lesions caused by enthesophytosis and the multiple bony proliferations at insertion sites of ligaments and tendons to appendicular bones in a lamellar or trabecular pattern were considered diagnostic features of the appendicular type of diffuse idiopathic skel-

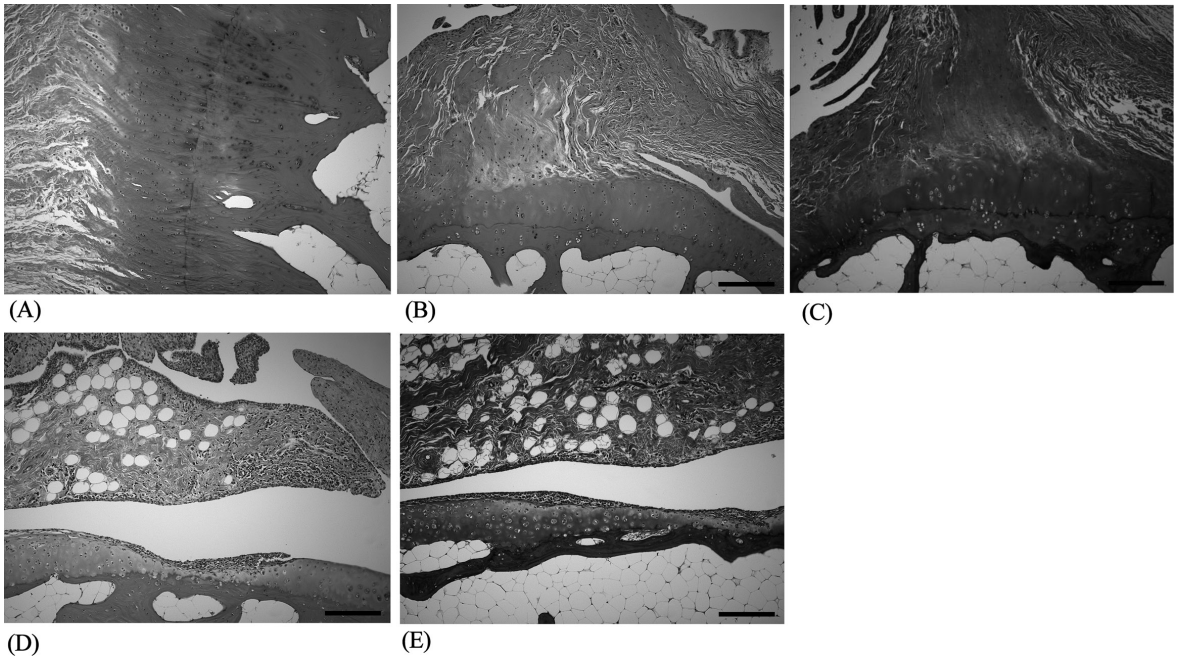

Fig. 5. Histopathologic findings of humerus. A rough and thickened periosteum was observed in the diaphysis and articular region. Osteoclasts were occassionally seen in the thickened periosteal are. Along them, osteoblasts were seen in the marginal area between periosteum and subchondral bone. Enthesophytes were observed, resulting in distinct separation from the cortical bone. 10X, H&E (A, B). Reactive bones along the margins of the humerus were merged into the meshwork of bundles of dense collagen framework. These collagens were arranged randomly and made a dense meshwork parallel to the articular surface. The deep zonal area showed irregular tidemark, calcified cartilage, mildly clustered chondrocytes and vascular invasion, indicating osteoarthritis. 100X, Masson's trichome staining (C). In the joint region, there was infiltration of lymphocytes and plasma cells as well as hypertrophy of the villi of the synovial membrane. Alongside of lymphocytic and plasma cells infiltrates was small blood vessels in the connective tissue. 10X, H&E (D). 100X, Masson's trichome staining (E).

etal hyperostosis. Diffuse idiopathic skeletal hyperostosis should be considered in the differential diagnosis when multiple enthesophytosis with a lamellar or trabecular pattern is observed in vertebrae as well as appendicular bone even in small breed dogs.

ACKNOWLEDGMENTS. This study was supported, in part, by a research grant from Chonnam National University, 2012 and by the Animal Medical Institute of Chonnam National University.

REFERENCES

1. Allan, G. 2013. Radiographic signs of joint disease in dogs and cats. p. 344. *In*: Textbook of Veterinary Diagnosic Radiology, 6th ed. (Thrall, D. E. ed.), Saunders Elsevier, St. Louis.
2. Kornmayer, M., Burger, M., Amort, K. and Brunnberg, L. 2013. Spinal fracture in a dog with diffuse idiopathic skeletal hyperostosis. *Vet. Comp. Orthop. Traumatol.* **26**: 76–81. [Medline] [CrossRef]
3. Kranenburg, H. C., Hazewinkel, H. A. and Meij, B. P. 2013. Spinal hyperostosis in humans and companion animals. *Vet. Q.* **33**: 30–42. [Medline] [CrossRef]
4. Kranenburg, H. C., Voorhout, G., Grinwis, G. C., Hazewinkel, H. A. W. and Meij, B. P. 2011. Diffuse idiopathic skeletal hyperostosis (DISH) and spondylosis deformans in purebred dogs: a retrospective radiographic study. *Vet. J.* **190**: e84–e90. [Medline] [CrossRef]
5. Kranenburg, H. C., Westerveld, L. A., Verlaan, J. J., Oner, F. C., Dhert, W. J. A., Voorhout, G., Hazewinkel, H. A. and Meij, B. P. 2010. The dog as an animal model for DISH? *Eur. Spine J.* **19**: 1325–1329. [Medline] [CrossRef]
6. Maddock, C. L., Wolbach, S. B. and Maddock, S. 1949. Hypervitaminosis A in the dog. *J. Nutr.* **39**: 117–137. [Medline]
7. Maertens, M., Mielants, H., Verstraete, K. and Veys, E. M. 1992. Evaluation of the involvement of axial entheses and sacroiliac joints in relation to diagnosis: comparison among diffuse idiopathic skeletal hyperostostis (DISH), osteoarthrosis and ankylosing spondylitis. *Clin. Rheumatol.* **11**: 551–557. [Medline] [CrossRef]
8. Morgan, J. P. S. 1991. Disseminated idiopathic skeletal hyperostosis (DISH) in a dogs. *Vet. Radiol.* **32**: 65–70. [CrossRef]
9. Ortega, M., Gonçalves, R., Haley, A., Wessmann, A. and Penderis, J. 2012. Spondylosis deformans and diffuse idiopathic skeletal hyperostosis (dish) resulting in adjacent segment disease. *Vet. Radiol. Ultrasound* **53**: 128–134. [Medline] [CrossRef]
10. Pollard, R. E. and Wisner, E. R. 2013. Orthopedic diseases of young and growing dogs and cats. pp. 275–276. *In*: Textbook of Veterinary Diagnosic Radiology, 6th ed. (Thrall, D. E. ed.), Saunders Elsevier, St. Louis.
11. Resnick, D., Shapiro, R. F., Wiesner, K. B., Niwayama, G., Utsinger, P. D. and Shaul, S. R. 1978. Diffuse idiopathic skeletal hyperostosis (DISH) [ankylosing hyperostosis of Forestier and Rotes-Querol]. *Semin. Arthritis Rheum.* **7**: 153–187. [Medline] [CrossRef]
12. Resnick, D., Shaul, S. R. and Robins, J. M. 1975. Diffuse idiopathic skeletal hyperostosis (DISH): Forestier's disease with extraspinal manifestations. *Radiology* **115**: 513–524. [Medline] [CrossRef]
13. Woodard, J. C., Poulos, P. W. Jr., Parker, R. B., Jackson, R. I. Jr. and Eurell, J. C. 1985. Canine diffuse idiopathic skeletal hyperostosis. *Vet. Pathol.* **22**: 317–326. [Medline]